Climate of the Past Discussions

Sea-ice dynamics strongly promote Snowball Earth initiation and destabilize tropical sea-ice margins

A. Voigt[1] and D. S. Abbot[2]

[1]Max Planck Institute for Meteorology, Hamburg, Germany
[2]University of Chicago, Illinois, USA

Correspondence to: A. Voigt (aiko.voigt@zmaw.de)

CPD

8, 2445–2475, 2012

Snowball Earth and sea-ice dynamics

A. Voigt and D. S. Abbot

Title Page	
Abstract	Introduction
Conclusions	References
Tables	Figures

◄◄	►►
◄	►
Back	Close

Full Screen / Esc

Printer-friendly Version

Interactive Discussion

Snowball Earth and sea-ice dynamics

A. Voigt and D. S. Abbot

Abstract

The Snowball Earth bifurcation, or runaway ice-albedo feedback, is defined for particular boundary conditions by a critical CO_2 and a critical sea-ice cover (SI), both of which are essential for evaluating hypotheses related to Neoproterozoic glaciations. Previous work has shown that the Snowball Earth bifurcation, denoted as $(CO_2, SI)^*$, differs greatly among climate models. Here, we revisit the initiation of a Snowball Earth in the atmosphere-ocean general circulation model ECHAM5/MPI-OM for Marinoan (~ 630 Ma) continents and solar insolation decreased to 94 %. In its standard setup, ECHAM5/MPI-OM initiates a Snowball Earth much more easily than other climate models at $(CO_2, SI)^* \approx (500\,\text{ppm}, 55\,\%)$. Previous work has shown that the Snowball Earth bifurcation can be pushed equatorward if a low bare sea ice albedo is assumed because bare sea ice is exposed by net evaporation in the descent region of the Hadley circulation. Consistent with this, when we replace the model's standard bare sea-ice albedo of 0.75 by a much lower value of 0.45, we find $(CO_2, SI)^* \approx (204\,\text{ppm}, 70\,\%)$. When we additionally disable sea-ice dynamics, we find that the Snowball Earth bifurcation can be pushed even closer to the equator and occurs at a much lower CO_2: $(CO_2, SI)^* \approx (2\,\text{ppm}, 85\,\%)$. Therefore, both lowering the bare sea-ice albedo and disabling sea-ice dynamics increase the critical sea-ice cover in ECHAM5/MPI-OM, but sea-ice dynamics have a much larger influence on the critical CO_2. For disabled sea-ice dynamics, the state with 85 % sea-ice cover is stabilized by the Jormungand mechanism and shares characteristics with the Jormungand climate states. However, there is no Jormungand bifurcation between this Jormungand-like state and states with mid-latitude sea-ice margins. Our results indicate that differences in sea-ice dynamics schemes can be as important as sea ice albedo for causing the spread in climate model's estimates of the location of the Snowball Earth bifurcation.

A. Voigt and D. S. Abbot

Discussion Paper | Discussion Paper | Discussion Paper | Discussion Paper | Discussion Paper

1 Introduction

The Neoproterozoic glaciations ($\sim$715 Ma and $\sim$630 Ma) are characterized by active, wide-spread continental glaciers in the tropics that reached down to sea level (Evans, 2000; Trindade and Macouin, 2007; Macdonald et al., 2010). Building on the runaway
ice-albedo feedback (e.g. Budyko, 1969; Sellers, 1969; Marotzke and Botzet, 2007) as well as the geology surrounding these glaciations, Kirschvink (1992) and Hoffman et al. (1998) proposed that Earth might have been in deep freeze with completely sea-ice covered oceans during these glaciations. Such climate states have become known as (hard) Snowball Earth.

From a climate dynamics point of view, one of the most important questions concerning the Snowball Earth hypothesis is the location of the bifurcation that is associated with the onset of the runaway ice-albedo feedback (i.e. the Snowball Earth bifurcation). The location of the Snowball Earth bifurcation is characterized by a critical sea-ice cover and a critical radiative forcing. The critical sea-ice cover is commonly measured
in per cent of the global ocean area; the critical radiative forcing is often expressed as a decrease in atmospheric CO_2 that is required to initiate a Snowball Earth when starting from a temperate climate with only partial sea-ice cover. In the following, we will denote the location of the Snowball Earth bifurcation as $(CO_2, SI)^*$.

Climate models have yielded different estimates for the critical CO_2. The
atmosphere-ocean general circulation model (AOGCM) ECHAM5/MPI-OM initiates a Snowball Earth for Marinoan ($\sim$635 Ma) continents and solar insolation (94 % of modern, 1285 W m^{-2}; Gough, 1981) when CO_2 is decreased to 500 ppm (Fig. 1)[1]. The easy Snowball initiation in ECHAM5/MPI-OM is in contrast to other climate models that experienced difficulties in triggering global sea-ice cover. For example, Chandler
and Sohl (2000), using the GISS atmosphere general circulation coupled to a slab ocean, and Poulsen et al. (2002), using the FOAM AOGCM, were unable to trigger

---

[1]Figure 1 contains a simulation with 500 ppm CO_2 that was run after Voigt et al. (2011) was published and hence was not included in Voigt et al. (2011).

a Snowball Earth, which sometimes is interpreted as an argument against the Snowball Earth hypothesis (Kennedy et al., 2001; Lubick, 2002; Kerr, 2010). Recently, Yang et al. (2012a,b,c) found that Snowball Earth initiation in the AOGCMs CCSM3 and CCSM4 requires 17.5 ppm and 70 ppm CO_2, respectively, with modern continents and

5   94 % solar constant. The CCSM3 and CCSM4 results are especially important because CCSM3, CCSM4, and ECHAM5/MPI-OM are all comprehensive atmosphere-ocean general circulation models, which sets them apart from other less sophisticated climate models that have been used to study Snowball initiation. Given the role of continents for Snowball initiation (Voigt et al., 2011), a comparison of the models'

10   CO_2 estimates is hampered by differences in the continental configurations. Nevertheless, ECHAM5/MPI-OM clearly initiates a Snowball much more easily than in particular CCSM3.

Similarly, climate models give different estimates of the critical sea-ice cover. The critical sea-ice cover is the maximum sea-ice cover of stable non-Snowball Earth states.

15   The critical sea-ice cover is important because the higher the critical sea-ice cover, the less one needs to invoke completely sea-ice covered oceans to explain the formation of tropical land glaciers. ECHAM5/MPI-OM has a critical sea-ice cover of 55 % (measured in per cent of the global ocean area), which appears to be too low to allow continental tropical ice sheets to co-exist with open tropical ocean since tropical land temperatures

20   remain well above freezing in this state (Voigt et al., 2011; Voigt and Marotzke, 2010). In contrast, CCSM3 has a critical sea-ice cover of 76 %, which might allow the growth of tropical ice sheets even though the ocean is not completely sea-ice covered (Yang et al., 2012a,b). Such states are usually referred to as soft Snowball Earth (Hyde et al., 2000; Liu and Peltier, 2010).

25   Sea-ice albedo is clearly an important control on the Snowball Earth bifurcation (Abbot et al., 2011; Pierrehumbert et al., 2011; Yang et al., 2012a). ECHAM5/MPI-OM in its standard configuration uses a high bare (snow-free) sea-ice albedo of 0.75, while CCSM3 uses a much smaller value of 0.50. This suggests that part of the reason the $(CO_2, SI)^*$ estimates of ECHAM5/MPI-OM and CCSM3 differ is differences in the

Snowball Earth and sea-ice dynamics

A. Voigt and D. S. Abbot

models' albedo of bare sea ice. Moreover, Abbot et al. (2011) proposed a new type of climate states, the so-called Jormungand climate states. The Jormungand states owe their existence to a strong albedo contrast between dark bare sea ice and highly reflective, snow-covered sea ice. Because descent of the Hadley circulation leads to net evaporation in the subtropics, the low albedo of bare sea ice allows the Jormungand states to have a sea-ice margin at $\approx 10°$ N/S, corresponding to sea-ice cover of more than 80 %. The high albedo contrast between bare and snow-covered sea ice leads to the Jormungand bifurcation and associated hysteresis, which separates the Jormungand states from states with less or no sea ice and make them a potentially important model for Neoproterozoic glaciations (see Abbot et al., 2011, for details). However, Abbot et al. (2011) only demonstrated the existence of Jormungand states in atmosphere-only aquaplanet simulations without ocean heat transport and sea-ice dynamics.

In this contribution, we revisit the initiation of a Marinoan Snowball Earth in ECHAM5/MPI-OM. We decrease the albedo of bare sea ice from its high standard value of 0.75 to a low value of 0.45. The simulations serve two purposes. First, by comparing these simulations to those with high bare sea-ice albedo (Voigt et al., 2011), we study how sensitive the $(CO_2, SI)^*$ estimate of ECHAM5/MPI-OM is to bare sea-ice albedo. Second, the new simulations allow us to test if Jormungand states also exist in a climate model with ocean dynamics, sea-ice dynamics and realistic continents. We will find that the critical CO_2 only modestly depends on the bare sea-ice albedo in ECHAM5/MPI-OM, so we also perform simulations with low bare sea-ice albedo and disabled sea-ice dynamics, as well as with ocean heat transport artificially set to zero. These further simulations demonstrate that sea-ice dynamics are critical for the Snowball Earth bifurcation and that disabling ocean dynamics has only a small effect if a low bare sea-ice albedo and no sea-ice dynamics are assumed.

The paper is organized as follows. We describe the atmosphere-ocean general circulation model ECHAM5/MPI-OM and the boundary conditions and simulation setup in Sect. 2. In Sect. 3, we present the simulations with the bare sea-ice albedo decreased

Snowball Earth and sea-ice dynamics

A. Voigt and D. S. Abbot

to 0.45. Motivated by an analysis of the tendencies of sea-ice thickness and snow on sea-ice, we then perform simulations with disabled sea-ice dynamics in addition to low bare sea-ice albedo. These are described in Sect. 4. Disabling sea-ice dynamics allows us to find a state with annual-mean sea-ice margin at 10° N/S. By further setting
5 ocean heat transport to zero, we show in Sect. 5 that ocean heat transport is not essential to the stability of the 10° N/S sea-ice margin. In Sect. 6, we show that the state with the 10° N/S sea-ice margin is not separated from states with less sea-ice cover by a Jormungand bifurcation. We give a general discussion of our results in Sect. 7, before concluding in Sect. 8.

10 **2   Model and simulation setup**

We apply the comprehensive atmosphere-ocean general circulation model, ECHAM5/MPI-OM. Apart from a change of the sea-ice albedo, this is the same model that we used to study the initiation of a modern (Voigt and Marotzke, 2010) as well as Marinoan Snowball Earth (Voigt et al., 2011). The model is described in detail in Voigt
15 and Marotzke (2010) and Voigt et al. (2011) and the references therein.

All simulations use modified albedo values for bare as well as snow-covered sea ice. Instead of the standard sea-ice albedo of ECHAM5/MPI-OM applied in Voigt et al. (2011) and Voigt and Marotzke (2010), we use the sea-ice albedo of the Community Atmosphere Model version 3 as given in Table 3 of Pierrehumbert et al. (2011), which
20 assumes 40 % of solar radiation at the surface is in the visible. Compared to the standard value, the modified bare sea-ice albedo is considerably lower; with a cold albedo of 0.45 instead of 0.75 (for surface temperatures below –1 °C), and a warm albedo of 0.38 instead of 0.55 (for surface temperatures at 0 °C; Fig. 2). The modified albedo of snow-covered sea-ice is nearly the same as ECHAM5/MPI-OM's standard value (warm
25 albedo of 0.66 instead of 0.65, cold albedo of 0.79 instead of 0.8; Fig. 2). Therefore, we consider the change in snow-covered sea-ice albedo not significant. As in the standard setup of ECHAM5/MPI-OM, the snow thickness that separates bare from snow-covered

sea-ice is 1 cm water equivalent (corresponding to a physical snow thickness of 3 cm), and there is no snow aging or spectral dependence of the sea-ice albedo.

ECHAM5/MPI-OM includes the zero-layer thermodynamic sea-ice model of Semtner (1976) with sea-ice dynamics following Hibler (1979). The sea-ice thermodynamics calculate the local sea-ice growth and melt. Snow on sea-ice is explicitly modeled, including snow/sea-ice conversion when the snow/sea-ice interface sinks below sea level because of heavy snow loading. The sea-ice thickness is limited to about 8 m to avoid dry ocean levels. The sea-ice dynamics scheme transports sea-ice thickness, sea-ice fraction, and snow on sea ice according to the prognosed sea-ice velocities. The sea-ice velocities are calculated based on the stresses of surface winds and ocean currents on sea ice, the Coriolis force, sea-surface tilt, and an assumed sea-ice rheology that describes internal deformation of sea ice. To study the role of sea-ice dynamics for Snowball Earth initiation, we disable sea-ice dynamics in some of the simulations.

Since it is an atmosphere-ocean general circulation model, ECHAM5/MPI-OM simulates the three-dimensional ocean circulation that is consistent with the modeled atmospheric state. The ocean circulation leads to ocean heat transport that can vary over time within a given simulation and differs between the simulations as a consequence of differences in the ocean circulation. For some simulations, we set the ocean heat transport to zero by reducing the ocean model to a single level of 50 m thickness and enforcing zero ocean velocities. We set ocean heat transport to zero only in combination with disabled sea-ice dynamics. The simulations with zero ocean heat transport apply exactly the same scheme sea-ice thermodynamical scheme as the other simulations.

We specify the same boundary conditions as in Voigt et al. (2011). These are meant to represent the Marinoan period (635 Million years before present) and include low-latitude desert continents with an albedo of 0.272. We use modern orbital parameters. Non-CO_2 well-mixed greenhouse gases are set to their pre-industrial concentrations ($CH_4 = 650$ ppb, $N_2O = 270$ ppb, no CFCs). Ozone follows the 1980–1991 climatology

of Fortuin and Kelder (1998), aerosols are specified according to Tanré et al. (1984). For a detailed list of the boundary conditions, see Voigt et al. (2011).

All simulations use a Marinoan solar constant of 1285 W m^{-2} (94 % of present-day value; Gough, 1981), while atmospheric CO_2 is varied. As in Voigt et al. (2011), we use an atmospheric resolution of spectral truncation T31 (corresponding to a horizontal grid distance of 3.75°) with 19 vertical levels. The ocean model uses 39 vertical levels and a curvilinear grid with horizontal resolution ranging from 50 km in equatorial regions to 435 km in parts of the Northern Hemisphere (see Voigt et al., 2011 for further details). All simulations use an atmosphere time step of 2400 s and an ocean time step of 3600 s.

3   Simulations with low bare sea-ice albedo of 0.45: $(CO_2, SI)^* \approx (204\,\text{ppm},\ 70\%)$

We begin with analyzing simulations with low bare sea-ice albedo of 0.45 but fully-active sea-ice dynamics and ocean heat transport. We generate a "warm" simulation for 1112 ppm CO_2 by restarting the model from the 1112 ppm CO_2 simulation with high bare sea-ice albedo of 0.75 (Fig. 3). As for a high bare sea-ice albedo, sea-ice cover settles around 40 % for 1112 ppm CO_2. For 1112 ppm CO_2, decreasing the bare sea-ice albedo thus only marginally affects the sea-ice cover. This is reasonable based on the fact that sea ice is restricted to latitudes poleward of 40° N/S, where it is snow-covered year-round except near the sea-ice margin during local summer.

Starting from 1112 ppm CO_2, we abruptly decrease CO_2 to determine the critical CO_2 (Fig. 3). Contrary to simulations with high bare sea-ice albedo, a decrease of CO_2 to pre-industrial levels (278 ppm) does not trigger a Snowball Earth. For 209 ppm, sea-ice cover equilibrates at 70 %, but a small further decrease of CO_2 to 204 ppm pitches the model into a Snowball state. Therefore, decreasing the bare sea-ice albedo from 0.75 to 0.45 allows us to find stable states with 70 % sea-ice cover instead of 55 % for high bare sea-ice albedo and makes Snowball initiation more difficult by lowering the critical CO_2 by a factor of 2.5 from 500 to 205 ppm. However, even with low bare sea-ice

albedo, Snowball Earth initiation does not require very low CO_2 and ECHAM5/MPI-OM still enters a Snowball Earth much more easily than the AOGCMs CCSM3 (Yang et al., 2012a,b) and FOAM (Poulsen and Jacob, 2004), although comparing the models is somewhat hampered by differences in the continental configurations.

Sea-ice dynamics offer a potential explanation for why the strong decrease in the bare sea-ice albedo has an only modest effect on Snowball Earth initiation in ECHAM5/MPI-OM. We diagnose the dynamical and thermodynamical sea-ice thickness tendencies in the simulation with 70 % sea-ice cover (209 ppm CO_2) and find large positive thickness tendencies due to sea-ice dynamics in the subtropics (Fig. 4). The annual-mean zonal-mean thickness tendency reaches a maximum of 1.5 cm day^{-1} at around 20° N/S (Fig. 4). The subtropical positive thickness tendency due to sea-ice dynamics is balanced by thermodynamical melting. In mid-latitudes, the role of sea-ice dynamics and thermodynamics are reversed, with sea ice growing by thermodynamics and being transported out of the mid-latitudes into the subtropics by sea-ice dynamics.

Given a sea-ice density of 910 kg m^{-3} and a sea-ice melting enthalpy of 330 × 10^3 J kg^{-1}, a sea-ice thickness tendency of 1 cm day^{-1} corresponds to a surface cooling of 35 W m^{-2}. Sea-ice dynamics are therefore important in cooling the latitudes equatorward of 30° N/S.

Associated with the transport of sea-ice thickness from mid- to low-latitudes, there is transport of snow on sea ice (Fig. 5). In the mid latitudes snow fall exceeds evaporation over ice, so mid-latitude sea ice is covered by snow at least 0.1 m thick (Fig. 5). When the mid-latitude sea ice is transported into the low latitudes, it carries snow on its top towards the equator. In low-latitudes, the snow gained through transport is balanced by a combination of snow melt and net evaporation. By virtue of the much higher albedo of snow-covered compared to bare sea ice, the snow transport contributes to the cooling of the low latitudes.

The latitude that separates snow-covered from bare sea-ice shows a strong seasonal migration, with low-latitude sea-ice being snow-covered during local winter and spring but bare during local summer and fall (Fig. 6). This migration results from the seasonal

cycle of the local snow melt, with strong melting in summer and fall and no melting in winter and spring. As sea-ice dynamics transport snow equatorward during all seasons, sea-ice is snow covered in winter and spring.

Overall, sea-ice dynamics cause large positive tendencies of sea-ice thickness and snow on sea-ice in the subtropics. This suggests that that sea-ice dynamics promote Snowball initiation and destabilize low-latitude sea-ice margins. We test this hypothesis in the following section.

4   Simulations with low bare sea-ice albedo of 0.45 and disabled sea-ice dynamics: $(CO_2, SI)^* \approx (2\,ppm, 85\,\%)$

We perform simulations with disabled sea-ice dynamics to test the hypothesis that sea-ice dynamics are important for Snowball Earth initiation in ECHAM5/MPI-OM. As in the previous section, these simulations use the low bare sea-ice albedo.

Figure 7 shows the time-evolution of sea-ice cover when sea-ice dynamics are disabled. The 139 ppm simulation starts from the 139 ppm simulation with low bare sea-ice albedo and active sea-ice dynamics. Without sea-ice dynamics, Snowball Earth initiation requires a decrease of CO_2 to 2 ppm. Disabling sea-ice dynamics hence lowers the critical CO_2 by a factor of 100 from 205 to 2 ppm, in line with the intuition built from the analysis of the sea-ice thickness and snow on sea-ice tendencies in Sect. 3. Hence, Snowball Earth initiation in ECHAM5/MPI-OM becomes very difficult when sea-ice dynamics are disabled.

Disabling sea-ice dynamics also shifts the runaway ice-albedo feedback to higher sea-ice cover and allows us to find a state with a stable sea-ice margin very close to the equator. For 4 ppm CO_2, sea-ice cover equilibrates at 85 %, corresponding to an annual-mean sea-ice margin at 10° N/S. (Fig. 8, right). During all months, sea-ice poleward of 20° N/S is covered by thick snow and has a high albedo, while sea-ice equatorward of 20° N/S is snow-free and has a low albedo. The low albedo of the bare sea ice weakens the ice-albedo feedback in low latitudes and allows the sea-ice margin to

Back | Close

Full Screen / Esc

Printer-friendly Version

Interactive Discussion

stabilize in the tropics. However, we emphasize that this tropical sea-ice margin is only possible in ECHAM5/MPI-OM when sea-ice dynamics and the associated equatorward transport of sea-ice and snow on sea-ice are disabled.

The separation of snow-covered from bare sea ice at 20° N/S is a consequence of the atmospheric hydrological cycle. Poleward of 20° N/S there is net accumulation of snow on sea ice, while evaporation over sea ice exceeds snow fall equatorward of 20° N/S (Fig. 8, middle). This hydrological pattern is consistent with the mean meridional circulation of the atmosphere. In particular, the subsiding branches of the Hadley cell are zones of net evaporation, which explains the jump in snow thickness and sea-ice albedo at 20° N/S. This confirms that the Jormungand mechanism of Abbot et al. (2011) for allowing a low-latitude sea-ice margin can work in a coupled AOGCM, albeit with disabled sea-ice dynamics in this case.

With the tropical sea-ice margin at 10° N/S, snow continuously accumulates on the continental regions around 30° N and 40° S. (Fig. 8, right). Annual-mean land temperatures are at or below 0 °C even at the equator, despite the uniform low continental elevation of 100 m. This suggests that with a tropical sea-ice margin, land glaciers could easily form in the more poleward parts of the continents, from where they could flow towards the equator.

It is commonly observed in models with ocean dynamics that ocean heat transport tends to converge heat to the sea-ice margin, thereby working against Snowball Earth initiation and stabilizing the sea-ice margin (Poulsen and Jacob, 2004; Ferreira et al., 2011; Voigt and Marotzke, 2010; Yang et al., 2012b). Indeed, in the 4 ppm simulation with tropical, 10° N/S sea-ice margin, shallow and narrow wind-driven ocean cells with strength of about 150 Sv converge about 10 W m^{-2} to the sea-ice margin. This raises the question whether ocean heat transport is essential to the stability of the tropical sea-ice margin.

5 Simulations with low bare sea-ice albedo of 0.45, disabled sea-ice dynamics, and zero ocean heat transport: $(CO_2, SI)^* \approx (4\,ppm, 85\,\%)$

We test the importance of ocean heat transport for Snowball initiation in ECHAM5/MPI-OM by performing simulations with ocean heat transport artificially set to zero. In all simulations presented in this section, the low bare sea-ice albedo is used and sea-ice dynamics are disabled.

Figure 9 presents time-series of the sea-ice cover for the simulations with zero ocean heat transport. Comparing these simulations to those with ocean heat transport at the same CO_2 level, we find that setting ocean heat transport to zero cools the climate and leads to a 10 % increase in sea-ice cover. For zero ocean heat transport, Snowball initiation requires a decrease of CO_2 to 4 ppm instead of 2 ppm with active ocean heat transport. In agreement with previous studies, ocean heat transport therefore works against Snowball initiation. However, additionally setting ocean heat transport to zero has a much smaller effect on the critical CO_2 than the previous disabling of sea-ice dynamics.

Also for ocean heat transport set to zero, we find a stable state with 85 % sea-ice cover and tropical sea-ice margin at 10° N/S. This demonstrates that the tropical sea-ice margin owes its stability to the low bare sea-ice albedo and not the ocean heat transport.

6 States with tropical sea-ice margin are not separated from states with mid-latitude sea-ice margins by Jormungand bifurcation

The state with 85 % sea-ice cover and a sea-ice margin at 10° N/S that we found when disabling sea-ice dynamics has properties that are characteristic for the Jormungand states described in Abbot et al. (2011). In particular, the sea-ice margin is very close to the equator, traces a serpent-like shape during the course of the year, and sea

ice equatorward of 20° N/S is bare year-round while sea-ice poleward of 20° N/S is constantly covered by thick snow (Fig. 8, left).

These properties suggest that the state with 85 % sea-ice cover might be a Jormungand state. If it was, then it would be separated from the states with less sea-ice cover by the Jormungand bifurcation and associated hysteresis. Put differently, when starting from the state with 85 % sea-ice cover and increasing CO_2, sea-ice cover would stay close to 85 % and would not retreat to the sea-ice cover that we find when approaching that CO_2 level from a warmer simulation with higher CO_2.

When CO_2 is increased from 4 to 9 ppm, sea-ice cover does not stay close to 85 % but decreases to 78 % within 600 yr, with no indication that the decrease in sea-ice cover during the last 100 yr is slower than during the first 100 yr following the CO_2 increase (Fig. 7). Similarly, when CO_2 is increased to 70 ppm, sea-ice cover shrinks quickly to 60 %. The lack of hysteresis indicates that the state with 85 % sea-ice cover is not separated from states with less sea-ice cover by a Jormungand bifurcation. This implies that the state with 85 % sea-ice cover belongs to the same equilibrium branch as the states with less sea-ice cover.

We ran analogous simulations with ocean heat transport set to zero (Fig. 9). Again, when we start from the state with 85 % sea-ice cover and increase CO_2 from 9 to 17, 70, or 278 ppm, respectively, we find no sign of the Jormungand bifurcation. This demonstrates that the lack of the Jormungand bifurcation in ECHAM5/MPI-OM is not caused by ocean dynamics and the associated ocean heat transport.

7 Discussion

In this contribution, we revisited Marinoan Snowball Earth initiation in the comprehensive atmosphere-ocean general circulation model ECHAM5/MPI-OM. The consequences of successively decreasing the bare sea-ice albedo from the model's high standard value of 0.75 to a low value of 0.45, disabling sea-ice dynamics, and finally setting ocean heat transport to zero are summarized in Fig. 10.

The Snowball bifurcation depends on sea-ice albedo, with lower sea-ice albedo postponing the bifurcation to lower CO_2 and higher sea-ice cover. Measurements suggest that a bare sea-ice albedo of 0.45 is more appropriate than 0.75 (Brandt et al., 1999, 2005; Warren et al., 2002), although the formation of hydrohalites at temperatures below $-23\,^\circ$C and the temperature-dependence of air bubble migration might increase the bare sea-ice albedo (Light et al., 2009; Dadic et al., 2010). For snow-covered sea-ice, measurements support an albedo of around 0.8 (Brandt et al., 2005; Warren et al., 2002), which is the value that we used in this study and that is commonly specified in climate models (Yang et al., 2012a). Decreasing the bare sea-ice albedo from 0.75 to 0.45 shifts Snowball Earth initiation to lower CO_2 and postpones the runaway ice-albedo feedback from 55 % to 70 % sea-ice cover. This is in qualitative agreement with Pierrehumbert et al. (2011) and Yang et al. (2012a). However, even for a bare sea-ice albedo of 0.45, Marinoan Snowball Earth initiation in ECHAM5/MPI-OM does not require very low CO_2 and ECHAM5/MPI-OM still enters a Snowball Earth much more easily than the atmosphere-ocean general circulation models CCSM3 (Yang et al., 2012a), CCSM4 (Yang et al., 2012c) and FOAM (Poulsen and Jacob, 2004), although comparing the models is hampered by differences in the boundary conditions. For example, given that the low-latitude Marinoan continents cool the climate (Voigt et al., 2011), part of the much lower critical CO_2 in CCSM3 and CCSM4 might be due to use of modern continents.

The rather small influence of bare sea-ice albedo on the Snowball Earth initiation behavior of ECHAM5/MPI-OM may be understood from sea-ice dynamics. Disabling sea-ice dynamics shifts the Snowball Earth bifurcation point from $(CO_2, SI)^* \approx (204\,\text{ppm}, 70\,\%)$ to $(4\,\text{ppm}, 85\,\%)$. The decrease of the critical CO_2 by a factor of 100 demonstrates that disabling sea-ice dynamics is the crucial step that turns ECHAM5/MPI-OM from a model that easily enters a Snowball Earth into a model that faces strong difficulties in Snowball Earth initiation. Sea-ice dynamics hence strongly promote Snowball Earth initiation by equatorward transport of sea ice and snow on sea ice. This result is in line with Lewis et al. (2007) and Yang et al. (2012a). Our results represent an

Snowball Earth and sea-ice dynamics

A. Voigt and D. S. Abbot

Back | Close

Full Screen / Esc

Printer-friendly Version

Interactive Discussion

A. Voigt and D. S. Abbot

important extension of these studies as we quantify the impact of sea-ice dynamics on the Snowball Earth bifurcation in an atmosphere-ocean general circulation model that in includes interactive surface winds. Note that in the model of Lewis et al. (2007), surface winds were prescribed.

With sea-ice dynamics disabled, we find a state with 85 % sea-ice cover and sea-ice margin at 10° N/S. In this state, sea-ice equatorward of 20° N/S is bare year-round, and the resulting weakening in the ice-albedo feedback allows the sea-ice margin to stabilize in the tropics. This state therefore owes its existence to the Jormungand mechanism described in Abbot et al. (2011) and shares characteristics with the Jormungand states. Because this state is not separated by a Jormungand bifurcation from states with less sea ice, this state is best described as a soft Snowball, "Slushball," or waterbelt state. The snow fall on land and annual-mean land surface temperatures close to or below freezing indicate that tropical glaciers could easily form in this state if our model included interactive land glaciers.

We do not find a Jormungand bifurcation in ECHAM5/MPI-OM. Ocean dynamics and associated ocean heat transport are not responsible for the absence of the Jormungand bifurcation. The fact that we do not find a Jormungand bifurcation in ECHAM5/MPI-OM does not exclude the possibility that other models might exhibit one. For example, hysteresis of the Jormungand state may be sensitive to the snow thickness that separates bare from snow-covered sea-ice, which is relatively small in ECHAM5/MPI-OM (1 cm water equivalent) compared to other models Pierrehumbert et al. (2011). Additionally, hysteresis may only be possible if extratropical sea ice can grow to large thicknesses (Jun Yang, personal communication, 2012), and the sea ice thickness is limited to 8 m in ECHAM5/MPI-OM. It is also possible that there are "hidden" Jormungand states that are not accessible due to, for example, a particular combination of the model's bare sea-ice albedo and efficiency of meridional heat transport (Abbot et al., 2011). Finally, the Jormungand bifurcation might be inhibited by the presence of continents.

Sea-ice dynamics strongly transport sea ice from mid- to low-latitudes. This transport pattern is reasonable given that the return flow of the Hadley cell leads to equatorward surface wind stress, which should drive sea ice toward the the subtropics. Additionally, thicker ice at mid-latitudes should viscously spread toward thinner ice in the subtropics.

5 Figuring out the main driver of the equatorward sea-ice transport requires an inspection of the sea-ice momentum budget. Such an inspection is beyond the scope of this study but is important to assess the role of the Hadley cell in stabilizing or destabilizing the subtropical sea-ice margin. Indeed, if the equatorward wind stress from the Hadley cell was the main driver, then the Hadley cell would at the same time give rise to the

10 stabilizing Jomrungand mechanism and the destablizing sea-ice dynamics mechanism.

The importance of sea-ice dynamics for Snowball Earth initiation calls for future work on sea-ice dynamics and their representation in climate models. For example, the viscous spread depends on an assumed sea-ice rheology. The rheology includes an ice-pressure term that causes thick ice to flow towards thin ice (see Hibler, 1979) and that

15 might be stronger in ECHAM5/MPI-OM compared to other climate models. A similar point of concern relates to the restriction of sea-ice thickness to 8 m in ECHAM5/MPI-OM, which inhibits the build-up of thick extratropical sea ice and the possible formation of sea glaciers (Goodman and Pierrehumbert, 2003; Tziperman et al., 2012). Finally, we note that even when two climate models used exactly the same sea-ice dynamics,

20 their simualted sea-ice dynamical tendencies could differ because of differences in the simulated surface winds and ocean circulation.

There are various reasons why climate models yield different estimates of the Snowball Earth bifurcation. Differences in the continental configuration (Voigt et al., 2011), sea-ice albedo (Pierrehumbert et al., 2011; Yang et al., 2012a), as well as clouds

25 and atmospheric dynamics (Pierrehumbert et al., 2011) are known to contribute to the spread. Because climate models differ in their representation of sea-ice dynamics, our results indicate that differences in sea-ice dynamics contribute substantially to the spread in climate-model estimates of the Snowball Earth bifurcation point. For example, the absence of sea-ice dynamics in FOAM likely is part of the reason why FOAM

experienced difficulties in entering a Snowball Earth (Poulsen et al., 2002; Poulsen, 2003; Poulsen and Jacob, 2004).

8 Conclusions

We revisit Marinoan Snowball Earth initiation in the comprehensive atmosphere-ocean general circulation model ECHAM5/MPI-OM. All simulations use a low bare sea-ice albedo of 0.45 that we adopt from the Community Atmosphere Model version 3 and that is much lower than the model's standard bare sea-ice albedo of 0.75 that we used in previous studies of Snowball initiation (Voigt et al., 2011; Voigt and Marotzke, 2010). For some simulations, we additionally disable sea-ice dynamics and set ocean heat transport to zero. We draw the following conclusions:

1. For the model's standard bare sea-ice albedo of 0.75, the Snowball Earth bifurcation point is $(CO_2, SI)^* \approx (500\,ppm, 55\,\%)$.

2. When the bare sea-ice albedo is decreased to 0.45, Snowball initiation becomes modestly more difficult and the bifurcation shifts to $(CO_2, SI)^* \approx (204\,ppm, 70\,\%)$.

3. Sea-ice dynamics lead to strong transport of sea-ice volume and snow on sea ice from mid- to low latitudes and thereby promote Snowball Earth initiation. When sea-ice dynamics are disabled in addition to a decrease of the bare sea-ice albedo, Snowball Earth initiation becomes very difficult and the Snowball Earth bifurcation is postponed to $(CO_2, SI)^* \approx (2\,ppm, 85\,\%)$.

4. For disabled sea-ice dynamics, we find a stable state with 85 % sea-ice cover. This state has a tropical sea-ice margin at 10° N/S and is enabled by the Jormungand mechanism described by Abbot et al. (2011): bare sea ice of low albedo is exposed when the sea ice margin reaches the descent region of the Hadley circulation. However, there is no Jormungand bifurcation and associated hysteresis that separates this state from states with mid-latitude sea-ice margins.

Full Screen / Esc

Printer-friendly Version

Interactive Discussion

5. The lack of Jormungand hysteresis is not caused by ocean dynamics and the associated ocean heat transport. Ocean heat transport is not essential in stabilizing the tropical 10° N/S sea-ice margin.

References

Abbot, D. S., Voigt, A., and Koll, D.: The Jormungand global climate state and implications for neoproterozoic glaciations, J. Geophys. Res., 116, D18103, doi:10.1029/2011JD015927, 2011. 2448, 2449, 2455, 2456, 2459, 2461

Brandt, R. E., Roesler, C. S., and Warren, S. G.: Spectral albedo, absorptance, and transmittance of Antarctic sea ice, in: Fifth Conference on Polar Meteorology and Oceanography, American Meteorological Society, Boston, 456–459, 1999. 2458

Brandt, R. E., Warren, S. G., Worby, A. P., and Grenfell, T. C.: Surface albedo of the antarctic sea ice zone, J. Climate, 18, 3606–3622, doi:10.1175/JCLI3489.1, 2005. 2458

Budyko, M. I.: Effect of solar radiation variations on climate of Earth, Tellus, 21, 611–619, 1969. 2447

Chandler, M. A. and Sohl, L. E.: Climate forcings and the initiation of low-latitude ice sheets during the Neoproterozoic Varanger glacial interval, J. Geophys. Res., 105, 20737–20756, 2000. 2447

Dadic, R., Light, B., and Warren, S. G.: Migration of air bubbles in ice under a temperature gradient, with application to "Snowball Earth", J. Geophys. Res., 115, D18125, doi:10.1029/2010JD014148, 2010. 2458

Evans, D. A. D.: Stratigraphic, geochronological, and paleomagnetic constraints upon the Neo-proterozoic climatic paradox, Am. J. Sci., 300, 347–433, doi:10.2475/ajs.300.5.347, 2000. 2447

Ferreira, D., Marshall, J., and Rose, B.: Climate determinism revisited: multiple equilibria in a complex climate model, J. Climate, 24, 992–1012, doi:10.1175/2010JCLI3580.1, 2011. 2455

Fortuin, J. P. F. and Kelder, H.: An ozone climatology based on ozonesonde and satellite mea-surements, J. Geophys. Res., 103, 31709–31734, doi:10.1029/1998JD200008, 1998. 2452

Goodman, J. C. and Pierrehumbert, R. T.: Glacial flow of floating marine ice in "Snowball Earth", J. Geophys. Res., 108, 3308, doi:10.1029/2002JC001471, 2003. 2460

Gough, D. O.: Solar interior structure and luminosity variations, Sol. Phys., 74, 21–34, doi:10.1007/BF00151270, 1981. 2447, 2452

Hibler, W. D.: Dynamic thermodynamic sea ice model, J. Phys. Oceanogr., 9, 815–846, 1979. 2451, 2460

Hoffman, P. F., Kaufman, A. J., Halverson, G. P., and Schrag, D. P.: A Neoproterozoic snowball earth, Science, 281, 1342–1346, doi:10.1126/science.281.5381.1342, 1998. 2447

Hyde, W. T., Crowley, T. J., Baum, S. K., and Peltier, W. R.: Neoproterozoic "snow-ball Earth" simulations with a coupled climate/ice-sheet model, Nature, 405, 425–429, doi:10.1038/35013005, 2000. 2448

Kennedy, M. J., Christie-Blick, N., and Sohl, L. E.: Are Proterozoic cap carbonates and isotopic excursions a record of gas hydrate destabilization following Earth's coldest intervals?, Geol-ogy, 29, 443–446, doi:10.1130/0091-7613(2001)029<0443:APCCAI>2.0.CO;2, 2001. 2448

Kerr, R. A.: Snowball Earth has melted back to a profound wintry mix, Science, 327, 1186, doi:10.1126/science.327.5970.1186, 2010. 2448

Kirschvink, J. L.: Late proterozoic low-latitude global glaciation: the snowball Earth, in: The Proterozoic Biosphere, Cambridge University Press, New York, 51–52, 1992. 2447

Lewis, J. P., Weaver, A. J., and Eby, M.: Snowball versus slushball Earth: dynamic versus non-dynamic sea ice?, J. Geophys. Res., 112, C11014, doi:10.1029/2006JC004037, 2007. 2458, 2459

Light, B., Brandt, R. E., and Warren, S. G.: Hydrohalite in cold sea ice: laboratory ob-servations of single crystals, surface accumulations, and migration rates under a tem-perature gradient, with application to "Snowball Earth", J. Geophys. Res., 114, C07018, doi:10.1029/2008JC005211, 2009. 2458

Snowball Earth and sea-ice dynamics

A. Voigt and D. S. Abbot

Title Page

Abstract	Introduction
Conclusions	References
Tables	Figures

| ◄◄ | ►► |
| ◄ | ► |

| Back | Close |

Full Screen / Esc

Printer-friendly Version

Interactive Discussion

Liu, Y. and Peltier, W. R.: A carbon cycle coupled climate model of Neoproterozoic glaciation: influence of continental configuration on the formation of a "soft snowball", J. Geophys. Res., 115, D17111, doi:10.1029/2009JD013082, 2010. 2448

Lubick, N.: Palaeoclimatology: snowball fights, Nature, 417, 12–13, doi:10.1038/417012a, 2002. 2448

Macdonald, F. A., Schmitz, M. D., Crowley, J. L., Roots, C. F., Jones, D. S., Maloof, A. C., Strauss, J. V., Cohen, P. A., Johnston, D. T., and Schrag, D. P.: Calibrating the cryogenian, Science, 327, 1241–1243, doi:10.1126/science.1183325, 2010. 2447

Marotzke, J. and Botzet, M.: Present-day and ice-covered equilibrium states in a comprehensive climate model, Geophys. Res. Lett., 34, L16704, doi:10.1029/2006GL028880, 2007. 2447

Pierrehumbert, R., Abbot, D., Voigt, A., and Koll, D.: Climate of the Neoproterozoic, Annu. Rev. Earth Pl. Sc., 39, 417–460, doi:10.1146/annurev-earth-040809-152447, 2011. 2448, 2450, 2458, 2459, 2460

Poulsen, C. J.: Absence of a runaway ice-albedo feedback in the Neoproterozoic, Geology, 31, 473–476, 2003. 2461

Poulsen, C. J. and Jacob, R. L.: Factors that inhibit snowball Earth simulation, Paleoceanography, 19, PA4021, doi:10.1029/2004PA001056, 2004. 2453, 2455, 2458, 2461

Poulsen, C. J., Jacob, R. L., Pierrehumbert, R. T., and Huynh, T. T.: Testing paleogeographic controls on a Neoproterozoic snowball Earth, Geophys. Res. Lett., 29, 1515, doi:10.1029/2001GL014352, 2002. 2447, 2461

Sellers, W. D.: A global climate model based on the energy balance of the Earth-atmosphere system, J. Appl. Meteorol., 8, 392–400, 1969. 2447

Semtner, A. J.: Model for thermodynamic growth of sea ice in numerical investigations of climate, J. Phys. Oceanogr., 6, 379–389, 1976. 2451

Tanré, D., Geleyn, J. F., and Slingo, J.: First results of the introduction of an advanced aerosol-radiation interaction in ECMWF low resolution global model, Deepak Publishing, Hampton, VA, USA, 133–177, 1984. 2452

Trindade, R. I. and Macouin, M.: Palaeolatitude of glacial deposits and palaeogeography of Neoproterozoic ice ages, C. R. Geosci., 339, 200–211, doi:10.1016/j.crte.2007.02.006, 2007. 2447

Snowball Earth and sea-ice dynamics

A. Voigt and D. S. Abbot

Back | Close

Full Screen / Esc

Printer-friendly Version

Interactive Discussion

Tziperman, E., Abbot, D. S., Ashkenazy, Y., Gildor, H., Pollard, D., Schoof, C. G., and Schrag, D. P.: Continental constriction and oceanic ice-cover thickness in a Snowball-Earth scenario, J. Geophys. Res., 117, C05016, doi:10.1029/2011JC007730, 2012. 2460

Voigt, A. and Marotzke, J.: The transition from the present-day climate to a modern Snowball Earth, Clim. Dynam., 35, 887–905, doi:10.1007/s00382-009-0633-5, 2010. 2448, 2450, 2455, 2461, 2467

Voigt, A., Abbot, D. S., Pierrehumbert, R. T., and Marotzke, J.: Initiation of a Marinoan Snowball Earth in a state-of-the-art atmosphere-ocean general circulation model, Clim. Past, 7, 249–263, doi:10.5194/cp-7-249-2011, 2011. 2447, 2448, 2449, 2450, 2451, 2452, 2458, 2460, 2461, 2466, 2467, 2475

Warren, S., Brandt, R. E., and McKay, C. P.: Snowball Earth: ice thickness on the tropical ocean, J. Geophys. Res., 107, 1–17, 2002. 2458

Yang, J., Peltier, W., and Hu, Y.: The initiation of modern "Soft Snowball" and "Hard Snowball" climates in CCSM3, Part 1: The influences of solar luminosity, CO_2 concentration, and the sea ice/snow albedo parameterization, J. Climate, 25, 2711–2736, doi:10.1175/JCLI-D-11-00189.1, 2012a. 2448, 2453, 2458, 2460

Yang, J., Peltier, W. R., and Hu, Y.: The Initiation of modern "Soft Snowball" and "Hard Snowball" climates in CCSM3, Part 2: Climate dynamic feedbacks, J. Climate, 25, 2737–2754, doi:10.1175/JCLI-D-11-00190.1, 2012b. 2448, 2453, 2455

Yang, J., Peltier, W. R., and Hu, Y.: The initiation of modern soft and hard Snowball Earth climates in CCSM4, Clim. Past, 8, 907–918, doi:10.5194/cp-8-907-2012, 2012c. 2448, 2458

Snowball Earth and sea-ice dynamics

A. Voigt and D. S. Abbot

Title Page

Abstract | Introduction

Conclusions | References

Tables | Figures

|◄ | ►|

◄ | ►

Back | Close

Full Screen / Esc

Printer-friendly Version

Interactive Discussion
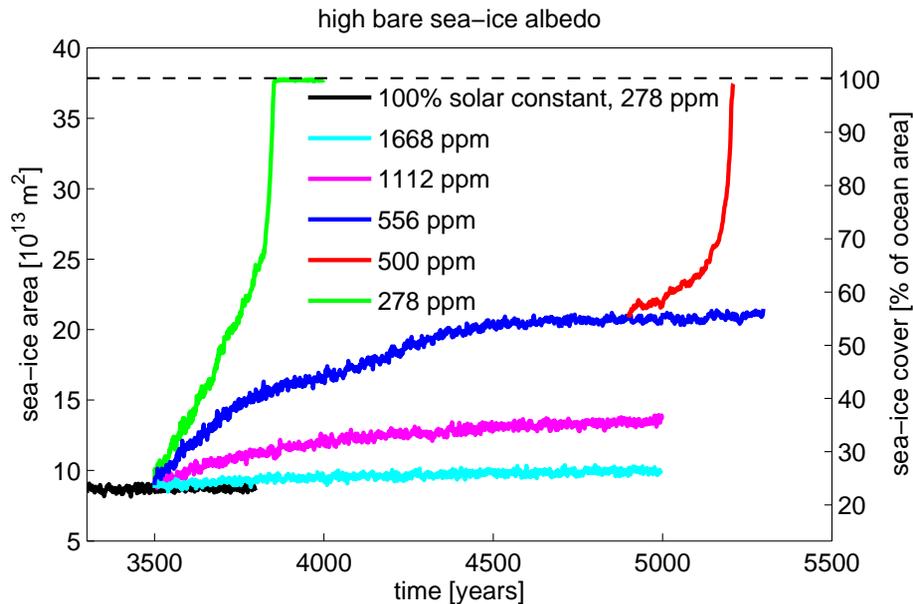
Fig. 1. Initiation of a Marinoan Snowball Earth in ECHAM5/MPI-OM with the model's standard high bare sea-ice albedo (Voigt et al., 2011). Time evolution of annual-mean global sea-ice cover in response to an abrupt decrease of the solar constant from 100 % to 94 % and a simultaneous increase of atmospheric carbon dioxide. Note that the simulation for 500 ppm CO_2 was run after Voigt et al. (2011) was published.

Full Screen / Esc

Printer-friendly Version

Interactive Discussion
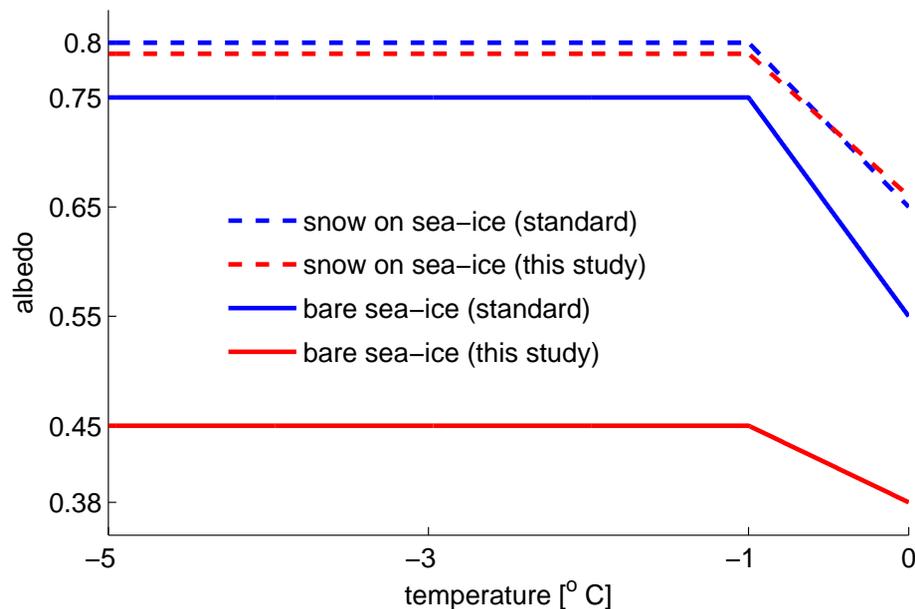
Fig. 2. Albedo of snow on sea ice (dashed) and bare sea ice (solid) of the standard setup of ECHAM5/MPI-OM used in Voigt et al. (2011) and Voigt and Marotzke (2010) (blue) and the values adopted from the Community Atmosphere Model version 3 used in this study (red).
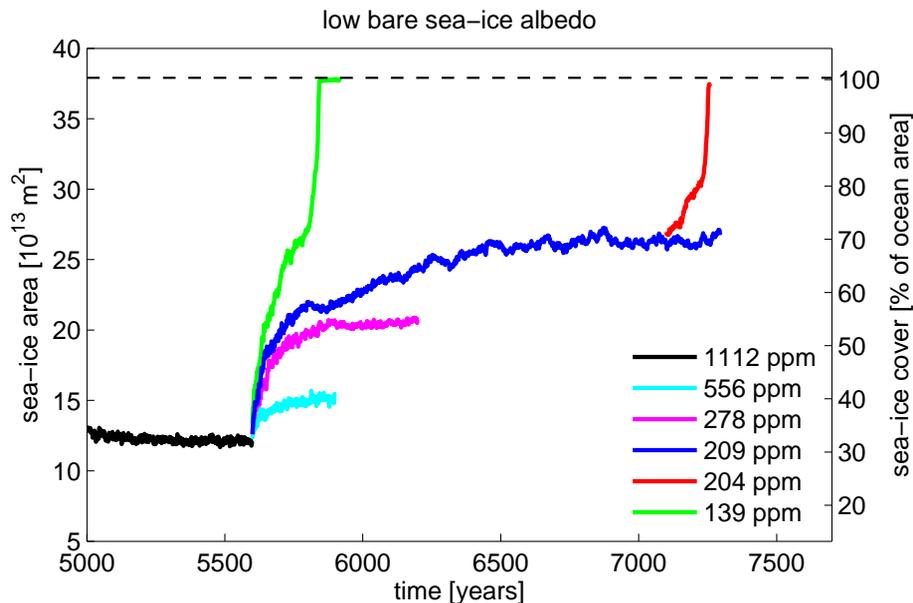
Fig. 3. Simulations with low bare sea-ice albedo. Time evolution of annual-mean global sea-ice cover in response to an abrupt change in CO_2. All simulations use 94 % solar insolation.

Title Page

Abstract | Introduction

Conclusions | References

Tables | Figures

◀ | ▶
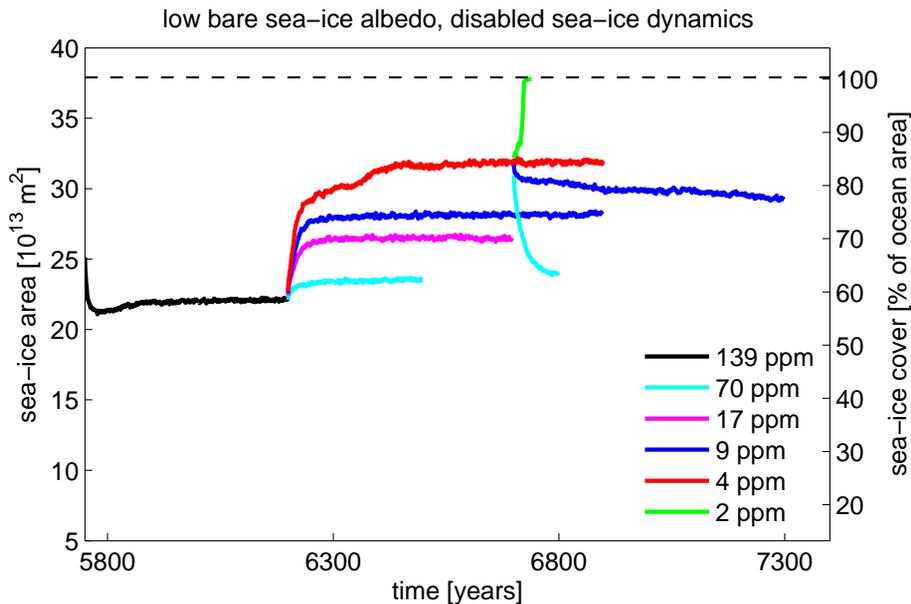
◀ | ▶

Back | Close

Full Screen / Esc

Printer-friendly Version

Interactive Discussion
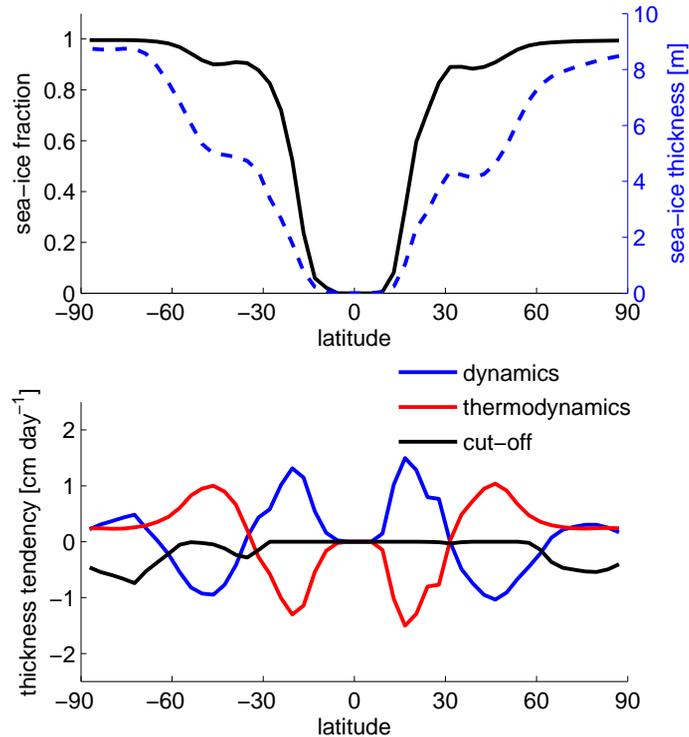
Fig. 4. Simulation with low bare-sea ice albedo and 209 ppm CO_2, which results in 70 % sea-ice cover. Top: zonal-mean annual-mean sea-ice fraction (black) and sea-ice thickness (blue). Bottom: zonal-mean annual-mean sea-ice thickness tendencies due to sea-ice dynamics (blue), sea-ice thermodynamics (red), and the cut-off of sea-ice thicker than 8 m (dotted black).
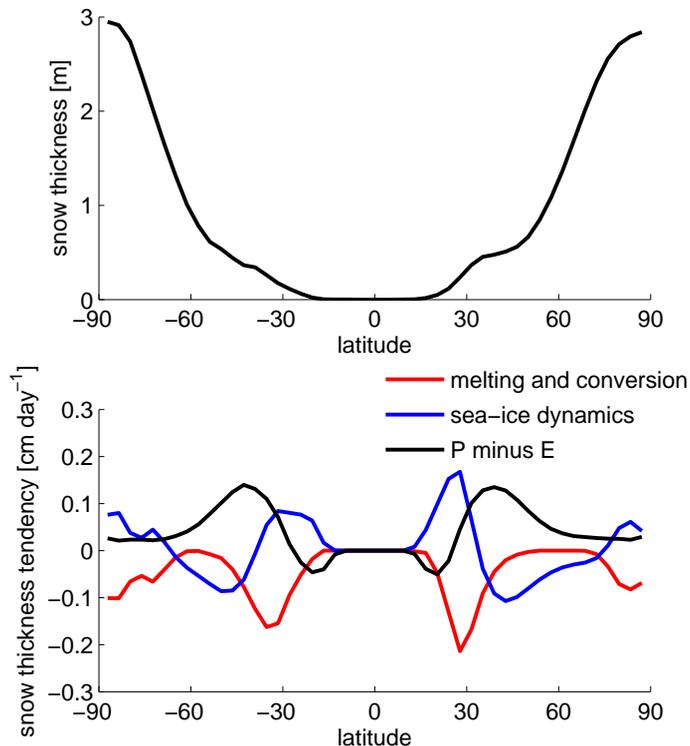
Fig. 5. Simulation with low bare-sea ice albedo and 209 ppm CO_2, which results in 70 % sea-ice cover. Top: zonal-mean annual-mean thickness of snow on sea ice. Bottom: zonal-mean annual-mean snow on sea-ice thickness tendencies due to local melting and snow/sea-ice conversion (blue), sea-ice dynamics (dashed red), and snowfall minus evaporation over sea ice (black).
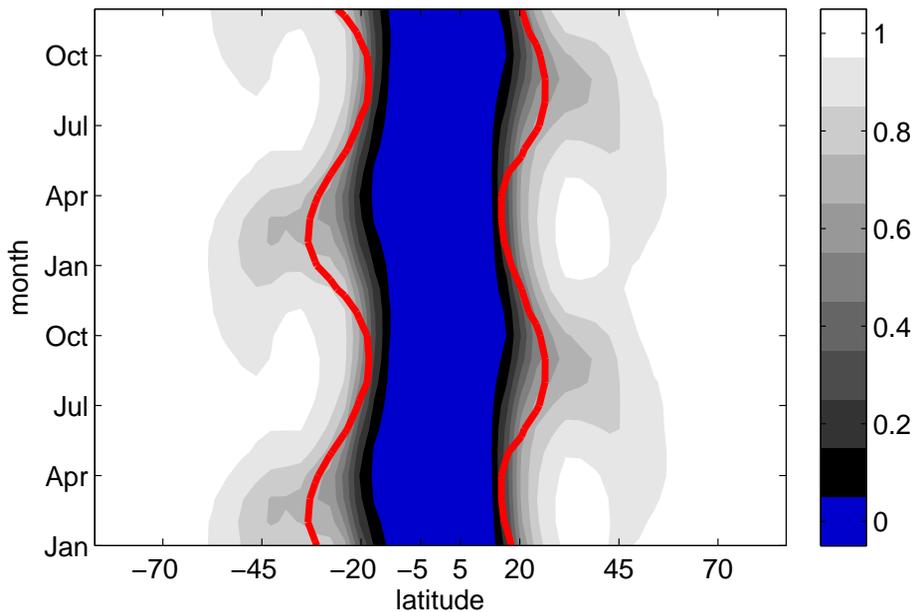
Fig. 6. Simulation with low bare-sea ice albedo and 209 ppm CO_2, which results in 70 % sea-ice cover. Annual cycle of zonal-mean sea-ice fraction. Blue indicates open ocean, white a sea-ice fraction of one (see color bar). Poleward of the red line, sea ice is snow-covered and hence highly reflective. Equatorward of the red line, sea ice is bare and hence comparably dark.

Fig. 7. Simulations with low bare sea-ice albedo and disabled sea-ice dynamics. Evolution of annual-mean global sea-ice cover in response to an abrupt change in CO_2 from a "warm" control simulation with 139 ppm CO_2. Also shown are simulations that start from the state with 85 % sea-ice cover and apply an abrupt increase of CO_2 from 4 ppm to various higher levels; these simulations search for the Jormungand bifurcation. All simulations use 94 % solar insolation.

Fig. 8. Simulation with low bare sea-ice albedo, disabled sea-ice dynamics, and 4 ppm CO_2. The simulation equilibrates at 85 % sea-ice cover. Left: seasonal cycle of zonal-mean sea-ice fraction. Blue indicates open ocean, white a sea-ice fraction of one (see color bar on the right). The red line separates bare sea ice (equatorward of the red line) from snow-covered sea-ice (poleward of the red line). Middle: Annual-mean zonal-mean snow fall onto sea ice minus evaporation over sea ice (black solid) and thickness of snow on sea ice (blue dashed). Right: annual-mean sea-ice fraction with the same color coding as in the left figure. The red line separates bare sea ice (equatorward of the red line) from snow-covered sea-ice (poleward of the red line). Continents are shown in brown. In the hatched continental regions snow accumulation exceeds $1\,\mathrm{cm}\,\mathrm{yr}^{-1}$.

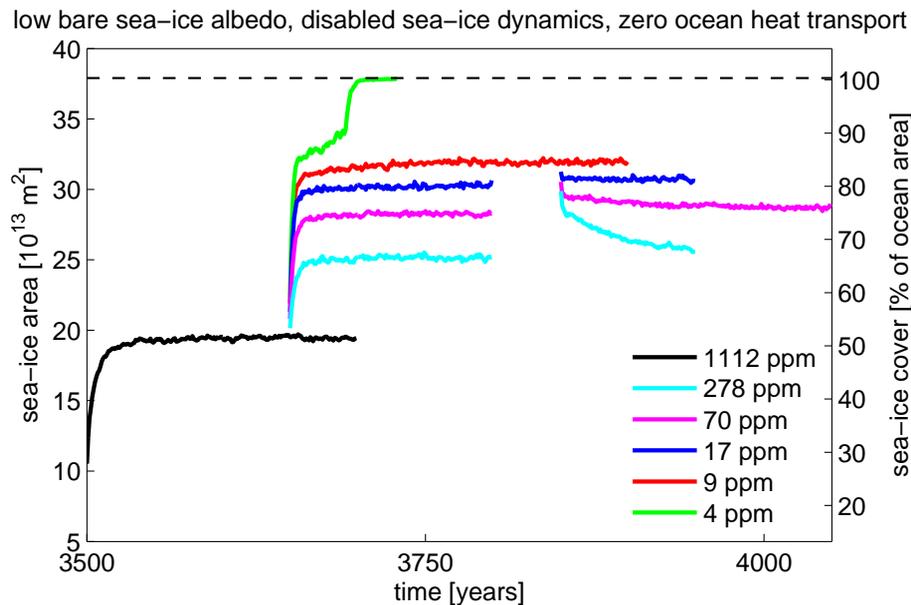low bare sea–ice albedo, disabled sea–ice dynamics, zero ocean heat transport

Fig. 9. Simulations with low bare sea-ice albedo, disabled sea-ice dynamics, and zero ocean heat transport. Evolution of annual-mean global sea-ice cover in response to an abrupt change in CO_2 from a "warm" control simulation with 1112 ppm CO_2. Also shown are simulations that start from the state with 85 % sea-ice cover and apply an abrupt increase of CO_2 from 9 ppm to various higher levels; these simulations search for the Jormungand bifurcation. All simulations use 94 % solar insolation.
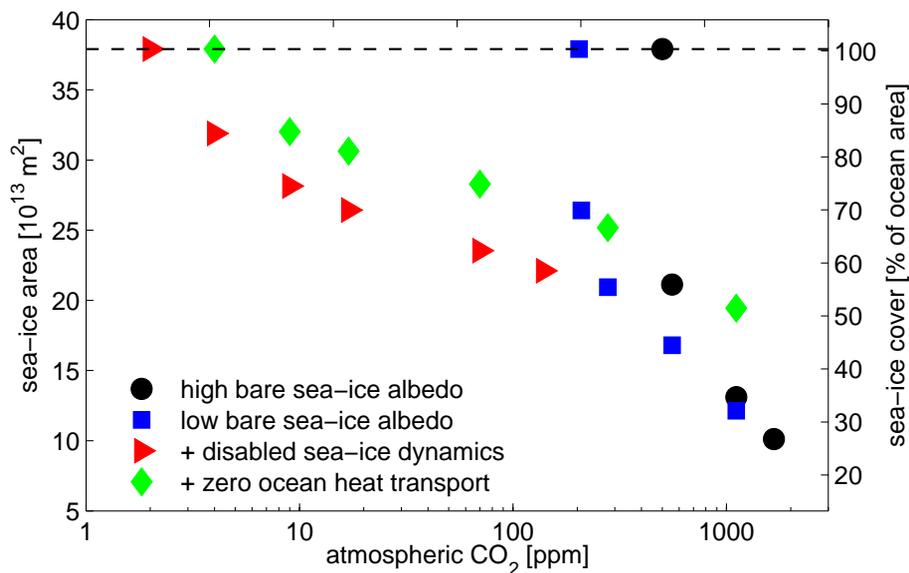
Fig. 10. Sea-ice cover as a function of CO_2 for simulations with high bare sea-ice albedo (black circles; Voigt et al., 2011), simulations with low bare sea-ice albedo (blue squares), simulations with low bare sea-ice albedo and disabled sea-ice dynamics (red triangles), and simulations with low bare sea-ice albedo, disabled sea-ice dynamics and zero ocean heat transport (green diamonds). All simulations use 94 % solar insolation.